A Calibration Method for Six-Accelerometer INS

Chao-Yu Hung and Sou-Chen Lee

Abstract: The gyroscope free strap-down INS is composed only of accelerometers. Any gyroscope free INS navigation error is deeply affected by the accuracy of the sensor bias, scale factor, orientation and location error. However these parameters can be found by calibration. There is an important research issue about a multi-position calibration method in this paper. It provides a novel method to find the error parameters for the six-accelerometer INS. A superior simulation is shown that the multi-position calibration can find the specifications of a six-accelerometer INS in laboratory. From these parameters the six-accelerometer INS could apply in realistic navigation.

Keywords: Bias, INS, multi-calibration, scale factor, strap-down.

1. INTRODUCTION

The first inertial navigation system (INS) was designed in 1948. The traditional INS uses the linear accelerometer to sense the linear acceleration and the gyroscope to measure the angular velocity. It is a self-contained system that the INS does not need other information or additional instrumentation [1,2]. A novel idea, angular velocity measurements without using gyros, was proposed by DiNapoli in 1965 [3]. In 1967, Schuler proposed the gyro-free strap-down scheme [4]. Schuler presumed a vehicle motion analysis requiring at least nine accelerometers. In theory, a minimum of six linear accelerometers is required for a complete description of a rigid body motion. In 1994, Chen and Lee was successful to present the six-accelerometer scheme [5]. The rotational and translatable accelerations of a vehicle were computed by using the accelerations of six accelerometers. The key to this scheme involved choosing the location and orientation of these accelerometers. This design scheme placed an accelerometer at each surface center of a cube, with the sensitive axis of each accelerometer aligned diagonally respective to the cube surface. In Chen's issue, the effect of gravity and attitude was ignored so that the six-accelerometer scheme can not apply on navigation.

The error effect is an important factor in INS. The orientation and location error are important error sources in a six-accelerometer INS. An error equation for the six-accelerometer scheme was proposed in Chen's paper. However, Chen did not display how the orientation and location error are produced. Among 1999-2002, Tan proposed a calibration method for a six-accelerometer INS [6-8]. It apply stationary test to find the orientation error. But it cannot get a unique solution. A multi-position calibration method is presented in this paper. The method is that dividing six accelerometers into two linearly independent sets and comparing the difference between ideal and real accelerometer output of each set through multi-position experiment in laboratory, the rotation and location error, bias, and scale factors can be obtained by numerical method. From these parameters the six-accelerometer INS could apply in realistic navigation.

2. THE SIX-ACCELEROMETER INS NAVIGATION EQUATION

The six-accelerometer configuration is shown in Fig. 1. In Fig. 1, we define the relationship between body-frame and inertial-frame as

- Point o_b denotes the geometric center which is the origin of the body-frame.
- ρ denotes the distance from the body-frame origin to each accelerometer.
- $\vec{\theta}_j$ represents the unit vector of the number j accelerometer in the sensitive axis.
- $\vec{\rho}_j$ represents the unit position vector of the number j accelerometer.

Manuscript received February 1, 2006; accepted June 5, 2006. Recommended by Editor Jae Weon Choi. This research was supported by the National Science Council, NSC-94-2212-E-262-005-. This support is gratefully acknowledged.

Chao-Yu Hung is with the Department of System Engineering, Chung Cheng Institute of Technology, National Defense University, Ta-shi, Tao-yuan County 335, Taiwan, R.O.C. (e-mail: g940405@ccit.edu.tw).

Sou-Chen Lee is with the College of Electrical Engineering and Computer Science, Lunghwa University of Science and Technology, 300, Sec. 1, Wanshou Rd., Gueishan Shiang, Tao-yuan County 333, Taiwan, R.O.C. (e-mail: sclee@mail.lhu.edu.tw).

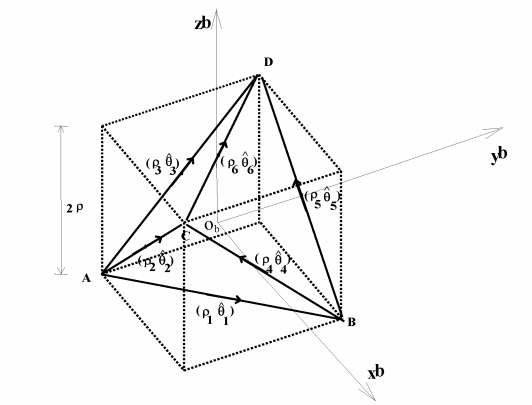

Fig. 1. Six-accelerometer scheme configuration.

Table 1. The position vector and sensitive vector of each accelerometer.

Acc. No.	Position vector	Sensitive vector
1	$\vec{\rho}_1^b = [0 \quad 0 \quad -\rho]^T$	$\vec{\theta}_1^b = \frac{1}{\sqrt{2}}[1 \quad 1 \quad 0]^T$
2	$\vec{\rho}_2^b = [0 \quad -\rho \quad 0]^T$	$\vec{\theta}_2^b = \frac{1}{\sqrt{2}}[1 \quad 0 \quad 1]^T$
3	$\vec{\rho}_3^b = [-\rho \quad 0 \quad 0]^T$	$\vec{\theta}_3^b = \frac{1}{\sqrt{2}}[0 \quad 1 \quad 1]^T$
4	$\vec{\rho}_4^b = [\rho \quad 0 \quad 0]^T$	$\vec{\theta}_4^b = \frac{1}{\sqrt{2}}[0 \quad -1 \quad 1]^T$
5	$\vec{\rho}_5^b = [0 \quad \rho \quad 0]^T$	$\vec{\theta}_5^b = \frac{1}{\sqrt{2}}[-1 \quad 0 \quad 1]^T$
6	$\vec{\rho}_6^b = [0 \quad 0 \quad \rho]^T$	$\vec{\theta}_6^b = \frac{1}{\sqrt{2}}[-1 \quad 1 \quad 0]^T$

The position vector and sensitive vector of each accelerometer are shown in Table 1. However in navigation application the position vector should be represented by inertial frame or body frame, which can be written as

- $\vec{R}^i$ denotes the position vector from O_I to point P, which is represented by the inertial frame.
- $\vec{r}^i$ denotes the position vector from O_I to o_b, which is represented by the inertial frame.
- $\vec{\rho}^b$ denotes the position vector from o_b to point P, which is represented by the body-frame.

Now we assume the six accelerometer INS fix on a vehicle and exercise on space. For convenience, we describe the accelerometer using the inertial-frame and body-frame. Let O_I represent the original point of the inertial coordinates and point P represents the accelerometer fixed into the body-frame. The geometry of the body-frame and inertial-frame is shown in Fig. 2. The six-accelerometer INS navigation equation is written as follows.

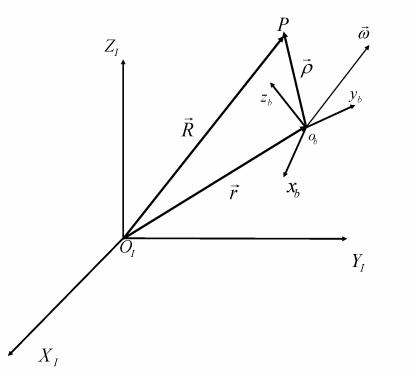

Fig. 2. Geometry of the body-frame (b) and inertial-frame (I).

The time derivative of the direction cosine matrix is [9]:

$$\dot{C}_b^i = C_b^i \left[\vec{\omega}_{ib}^b \times \right], \tag{1}$$

where $C_b^i(t)$ is a transformation matrix, transforming a column matrix from body coordinates into inertial coordinates.

- The position equation is

$$\dot{\vec{r}}^i = C_b^i \left(\vec{v}^b + \vec{\omega}_{ib}^b \times \vec{r}^b \right). \tag{2}$$

- The velocity equation is

$$\dot{\vec{v}}^i = C_b^i \left(\frac{1}{2} TA + \rho \begin{bmatrix} \omega_y \omega_z \\ \omega_x \omega_z \\ \omega_x \omega_y \end{bmatrix} \right), \tag{3}$$

where

$$A = [A_1 \quad A_2 \quad A_3 \quad A_4 \quad A_5 \quad A_6]^T,$$

$$A_j = s_j + C_i^b \vec{G}^i \cdot \vec{\theta}_j; \; j = 1, \cdots, 6,$$

s_j is accelerometer measurement output,

$$T = \frac{1}{\sqrt{2}} \begin{bmatrix} 1 & 1 & 0 & 0 & -1 & -1 \\ 1 & 0 & 1 & -1 & 0 & 1 \\ 0 & 1 & 1 & 1 & 1 & 0 \end{bmatrix}.$$

- The angular velocity equation is

$$\dot{\vec{\omega}}_{ib}^b = \frac{1}{2} S \big/ \rho \cdot A, \tag{4}$$

where

$$S = \frac{1}{\sqrt{2}} \begin{bmatrix} 1 & -1 & 0 & 0 & 1 & -1 \\ -1 & 0 & 1 & -1 & 0 & -1 \\ 0 & 1 & -1 & -1 & 1 & 0 \end{bmatrix}.$$

3. THE ORIENTATION CALIBRATION OF THE SIX-ACCELEROMETER SCHEME

The navigation errors of the strap-down six-accelerometer INS involve the sensor's bias, scale factor and initial alignment accuracy. For instance, a six-accelerometer INS with measurement error 1min-g causes the angular velocity errors about 0.02 rad/s in 10 seconds, which showed as Fig. 3. And it causes the linear velocity errors about ± 4 m/s in 10 seconds, which showed as Fig. 4.

In Fig. 3, the angular velocity errors are about proportional to t. In Fig. 4, the linear velocity errors are about proportional to t^3. It fits the result of Chen's. Because the gravity acts on each accelerometer in the six-accelerometer scheme in different attitudes, the orientation error, bias and scale factor of each accelerometer will be determined by using the orientation calibration. The key element in orientation calibration is that the accelerometers sensitive axes must be linearly independent. We divide six accelerometers into two sets that are linearly independent, and calibrate each set. The sensitive

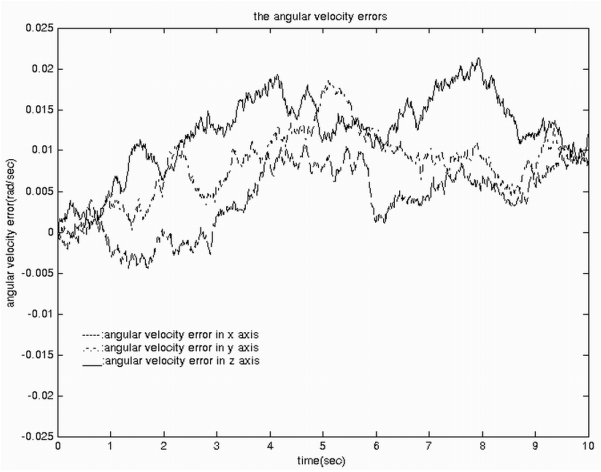

Fig. 3. The vehicle angular velocity errors.

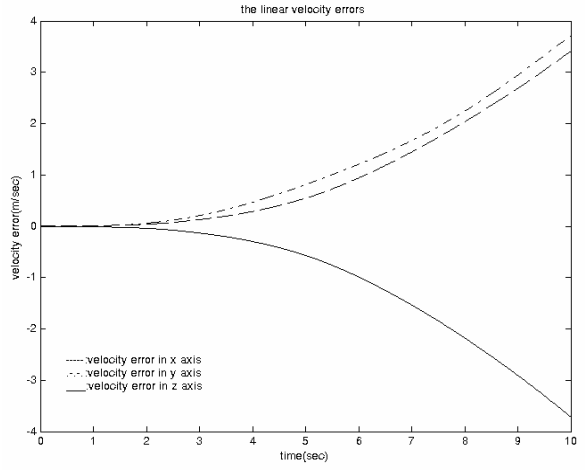

Fig. 4. The vehicle linear velocity errors.

Table 2. Linearly independent six accelerometer sets.

$\left[\vec{\theta}_1^b \quad \vec{\theta}_2^b \quad \vec{\theta}_5^b\right]$;	$\left[\vec{\theta}_3^b \quad \vec{\theta}_4^b \quad \vec{\theta}_6^b\right]$
$\left[\vec{\theta}_1^b \quad \vec{\theta}_2^b \quad \vec{\theta}_6^b\right]$;	$\left[\vec{\theta}_3^b \quad \vec{\theta}_4^b \quad \vec{\theta}_5^b\right]$
$\left[\vec{\theta}_2^b \quad \vec{\theta}_3^b \quad \vec{\theta}_4^b\right]$;	$\left[\vec{\theta}_1^b \quad \vec{\theta}_5^b \quad \vec{\theta}_6^b\right]$
$\left[\vec{\theta}_1^b \quad \vec{\theta}_3^b \quad \vec{\theta}_4^b\right]$;	$\left[\vec{\theta}_2^b \quad \vec{\theta}_5^b \quad \vec{\theta}_6^b\right]$
$\left[\vec{\theta}_1^b \quad \vec{\theta}_3^b \quad \vec{\theta}_6^b\right]$;	$\left[\vec{\theta}_2^b \quad \vec{\theta}_4^b \quad \vec{\theta}_5^b\right]$
$\left[\vec{\theta}_2^b \quad \vec{\theta}_3^b \quad \vec{\theta}_5^b\right]$;	$\left[\vec{\theta}_1^b \quad \vec{\theta}_4^b \quad \vec{\theta}_6^b\right]$

axes of six accelerometers show in Table 1 and the linearly independent sets depicted in Table 2. In this paper, the orientation calibration selects the set $\left[\vec{\theta}_2^b \quad \vec{\theta}_3^b \quad \vec{\theta}_5^b\right]$, $\left[\vec{\theta}_1^b \quad \vec{\theta}_4^b \quad \vec{\theta}_6^b\right]$ to do.

3.1. Determining the number #2, #3, and #5 accelerometers parameters

Let the ideal sensitive axis of each accelerometer be $\vec{\theta}_j^a;\ j=1\cdots 6,$ the true sensitive axis is $\vec{\theta}_j^{a'}$ and an acceleration of $\vec{a}^b=\left[a_x \quad a_y \quad a_z\right]^T$ in the body coordinate. The relation between the acceleration of each accelerometer in the true sensitive axis and the ideal sensitive axis can be written as

$$\vec{a}^{a'} = C_a^{a'} C_b^a \vec{a}^b. \tag{5}$$

In above equation the $C_a^{a'}$ is a transformation matrix that relates the ideal sensitive axes to the true sensitive axes, defined as

$$C_a^{a'} = \begin{bmatrix} 1 & \Delta\beta_{xz} & -\Delta\beta_{xy} \\ -\Delta\beta_{yz} & 1 & \Delta\beta_{yx} \\ \Delta\beta_{zy} & -\Delta\beta_{zx} & 1 \end{bmatrix}. \tag{6}$$

The other transformation matrix C_b^a relates the body coordinate to the ideal sensitive axes, defined as

$$C_b^a = \frac{1}{\sqrt{2}} \begin{bmatrix} 1 & 0 & 1 \\ 0 & 1 & 1 \\ -1 & 0 & 1 \end{bmatrix}. \tag{7}$$

The measured outputs of the accelerometers are determined by substituting equations (6) and (7) into (5). However the accelerometer outputs are expressed as an analog electric signal which involves a scale factor SF_{aj} and bias b_{aj} so that we express them as (8) that are

$$P_{a2} = SF_{a2}(T)\int_0^T \left(b_{a2}(T) + \frac{1}{\sqrt{2}}\left[\left(1+\Delta\beta_{xy}\right)a_x^b + \Delta\beta_{xz}a_y^b + \left(1+\Delta\beta_{xz}-\Delta\beta_{xy}\right)a_z^b \right] \right) dt, \quad (8a)$$

$$P_{a3} = SF_{a3}(T)\int_0^T \left(b_{a3}(T) + \frac{1}{\sqrt{2}}\left[-\left(\Delta\beta_{yz}+\Delta\beta_{yx}\right)a_x^b + a_y^b + \left(1+\Delta\beta_{yx}-\Delta\beta_{yz}\right)a_z^b \right] \right) dt, \quad (8b)$$

$$P_{a5} = SF_{a5}(T)\int_0^T \left(b_{a5}(T) + \frac{1}{\sqrt{2}}\left[-\left(1-\Delta\beta_{zy}\right)a_x^b - \Delta\beta_{zx}a_y^b + \left(1-\Delta\beta_{zx}+\Delta\beta_{zy}\right)a_z^b \right] \right) dt. \quad (8c)$$

The error parameters, scale factor, biases, orientation and location error, can be determined by using a multi-position static test. Since there are twelve unknown parameter should determine, it need at least six positions to generate eighteen output equations through (8) to determine the parameters for the number #2, #3, and #5 accelerometers. The six positions allow the input axis of the accelerometers to be pointed upwards and downwards once. The three gravity components along the body axes in the six positions are shown in Table 3.

Substituting gravity, as shown in Table 3, into (8), we can obtain the output equations P_{aij}; where the index represents the measured output from the number i accelerometer due to the gravity on j along the body axes. There are eighteen equations of output equations P_{aij} that can find the scale factors, bias and orientation error.

Table 3. The gravity of the #2, #3, and #5 accelerometers.

No.	Gravity acceleration
1	$\vec{a}_{b1} = \frac{g}{\sqrt{2}}\begin{bmatrix}-1 & 0 & 1\end{bmatrix}^T$
2	$\vec{a}_{b2} = -\frac{g}{\sqrt{2}}\begin{bmatrix}-1 & 0 & 1\end{bmatrix}^T$
3	$\vec{a}_{b3} = \frac{g}{\sqrt{2}}\begin{bmatrix}1 & 0 & 1\end{bmatrix}^T$
4	$\vec{a}_{b4} = -\frac{g}{\sqrt{2}}\begin{bmatrix}1 & 0 & 1\end{bmatrix}^T$
5	$\vec{a}_{b5} = \frac{g}{\sqrt{2}}\begin{bmatrix}0 & 1 & 1\end{bmatrix}^T$
6	$\vec{a}_{b6} = -\frac{g}{\sqrt{2}}\begin{bmatrix}0 & 1 & 1\end{bmatrix}^T$

Table 4. The gravity of the #1, #4, and #6 accelerometers.

No.	Gravity acceleration
1	$\vec{a}_{b1} = \frac{g}{\sqrt{2}}\begin{bmatrix}0 & -1 & 1\end{bmatrix}^T$
2	$\vec{a}_{b2} = -\frac{g}{\sqrt{2}}\begin{bmatrix}0 & -1 & 1\end{bmatrix}^T$
3	$\vec{a}_{b3} = \frac{g}{\sqrt{2}}\begin{bmatrix}1 & 1 & 0\end{bmatrix}^T$
4	$\vec{a}_{b4} = -\frac{g}{\sqrt{2}}\begin{bmatrix}1 & 1 & 0\end{bmatrix}^T$
5	$\vec{a}_{b5} = \frac{g}{\sqrt{2}}\begin{bmatrix}-1 & 1 & 0\end{bmatrix}^T$
6	$\vec{a}_{b6} = -\frac{g}{\sqrt{2}}\begin{bmatrix}-1 & 1 & 0\end{bmatrix}^T$

3.2. Determining the number #1, #4, and #6 accelerometers parameters

In the same way, let the transformation matrix be defined as

$$C_a^{a'} = \begin{bmatrix} 1 & \Delta\alpha_{xz} & -\Delta\alpha_{xy} \\ -\Delta\alpha_{yz} & 1 & \Delta\alpha_{yx} \\ \Delta\alpha_{zy} & -\Delta\alpha_{zx} & 1 \end{bmatrix}. \quad (9)$$

The transformation matrix that relates the body coordinates to the ideal sensitive axes are

$$C_b^a = \frac{1}{\sqrt{2}}\begin{bmatrix} 1 & 0 & 1 \\ 0 & 1 & 1 \\ -1 & 0 & 1 \end{bmatrix}. \quad (10)$$

The accelerometer output pulses with scale factor SF_{aj} and bias b_{aj} can be determined. The three gravity components along the body axes in the six positions for the number #1, #4, and #6 accelerometers are shown in Table 4. There are eighteen equations are generated, and the scale factors, bias and orientation error can be found by these equations.

4. THE LOCATION CALIBRATION OF THE SIX-ACCELEROMETER SCHEME

The location error $\Delta\vec{\rho}_j$ is one of the navigation errors. It will affect the accuracy of the velocity equation (3) and angular velocity equation (4). The location error causes the error of centripetal force in rotation motion with constant angular rate. Thus the location error can be determined by comparing the

ideal and real centripetal force. Assuming the real position vectors $\vec{\rho}_j^*$ of each accelerometer is

$$\vec{\rho}_j^* = \vec{\rho}_j + \Delta\vec{\rho}_j. \tag{11}$$

The error position $\Delta\vec{\rho}_j$ represents as

$$\Delta\vec{\rho}_j = \begin{bmatrix} \Delta x_j & \Delta y_j & \Delta z_j \end{bmatrix}^T;\ j = 1\cdots 6.$$

We generate three centripetal forces for each accelerometer through rotating the six-accelerometer scheme order the x, y and z axes respectively. After comparing the differences between the ideal measured output and the real one, we obtain the location error. By centripetal force, the specific force of each accelerometer can be determined, which is

$$\vec{f}_j^{b*} = \vec{\omega}_{ib}^b \times \vec{\omega}_{ib}^b \times \vec{\rho}_j^{b*} - C_i^b \vec{G}^i. \tag{12}$$

The output s_j^* of each accelerometer is determined. Setting three angular rates are

$$\vec{\omega}_x = \begin{bmatrix} \omega_x & 0 & 0 \end{bmatrix}^T,\ \vec{\omega}_y = \begin{bmatrix} 0 & \omega_y & 0 \end{bmatrix}^T,\ \vec{\omega}_z = \begin{bmatrix} 0 & 0 & \omega_z \end{bmatrix}^T.$$

The pulses P_{aj} are shown in Table 5. Each accelerometer has three equations shown. We can determine the location errors by using these equations.

5. THE CALIBRATION SIMULATION FOR A SIX-ACCELEROMETER INS

The calibration simulation will help us verify proposed calibration method of six-accelerometer INS.

Table 5. The accelerometer output pulses of six-accelerometer scheme.

Number	The accelerometer output pulses due to angular velocity
1	$P_{a1x} = SF_{a1}(T)\int_0^T \left(b_{a1}(T) + \frac{1}{\sqrt{2}} \begin{bmatrix} -G(1+\Delta\alpha_{xy}) - \omega_x^2 \Delta y_1 (1 - \Delta\alpha_{xy} - \Delta\alpha_{xz}) - \\ \omega_x^2 (-\rho + \Delta z_1)\Delta\alpha_{xz} \end{bmatrix} \right) dt$ $P_{a1y} = SF_{a1}(T)\int_0^T \left(b_{a1}(T) + \frac{1}{\sqrt{2}} \begin{bmatrix} -\omega_y^2 \Delta x_1 (1+\Delta\alpha_{xy}) - G(1 - \Delta\alpha_{xy} - \Delta\alpha_{xz}) - \\ \omega_y^2 (-\rho + \Delta z_1)\Delta\alpha_{xz} \end{bmatrix} \right) dt$ $P_{a1z} = SF_{a1}(T)\int_0^T \left(b_{a1}(T) + \frac{1}{\sqrt{2}} \begin{bmatrix} -\omega_z^2 \Delta x_1 (1+\Delta\alpha_{xy}) - \\ \omega_z^2 \Delta y_1 (1 - \Delta\alpha_{xy} - \Delta\alpha_{xz}) - G\Delta\alpha_{xz} \end{bmatrix} \right) dt$
2	$P_{a2x} = SF_{a2}(T)\int_0^T \left(b_{a2}(T) + \frac{1}{\sqrt{2}} \begin{bmatrix} -G(1+\Delta\beta_{xy}) - \omega_x^2 (-\rho + \Delta y_2)\Delta\beta_{xz} - \\ \omega_x^2 \Delta z_2 (1 + \Delta\beta_{xz} - \Delta\beta_{xy}) \end{bmatrix} \right) dt$ $P_{a2y} = SF_{a2}(T)\int_0^T \left(b_{a2}(T) + \frac{1}{\sqrt{2}} \begin{bmatrix} -\omega_y^2 \Delta x_2 (1+\Delta\beta_{xy}) - G\Delta\beta_{xz} - \\ \omega_y^2 \Delta z_2 (1 + \Delta\beta_{xz} - \Delta\beta_{xy}) \end{bmatrix} \right) dt$ $P_{a2z} = SF_{a2}(T)\int_0^T \left(b_{a2}(T) + \frac{1}{\sqrt{2}} \begin{bmatrix} -\omega_z^2 \Delta x_2 (1+\Delta\beta_{xy}) - \omega_z^2 (-\rho + \Delta y_2)\Delta\beta_{xz} - \\ G(1 + \Delta\beta_{xz} - \Delta\beta_{xy}) \end{bmatrix} \right) dt$
3	$P_{a3x} = SF_{a3}(T)\int_0^T \left(b_{a3}(T) + \frac{1}{\sqrt{2}} \begin{bmatrix} G(\Delta\beta_{yz} + \Delta\beta_{yx}) - \omega_x^2 \Delta y_3 - \\ \omega_x^2 \Delta z_3 (1 + \Delta\beta_{yx} - \Delta\beta_{yz}) \end{bmatrix} \right) dt$ $P_{a3y} = SF_{a3}(T)\int_0^T \left(b_{a3}(T) + \frac{1}{\sqrt{2}} \begin{bmatrix} \omega_y^2 (-\rho + \Delta x_3)(\Delta\beta_{yz} + \Delta\beta_{yx}) - G - \\ \omega_y^2 \Delta z_3 (1 + \Delta\beta_{yx} - \Delta\beta_{yz}) \end{bmatrix} \right) dt$ $P_{a3z} = SF_{a3}(T)\int_0^T \left(b_{a3}(T) + \frac{1}{\sqrt{2}} \begin{bmatrix} \omega_z^2 (-\rho + \Delta x_3)(\Delta\beta_{yz} + \Delta\beta_{yx}) - \omega_z^2 \Delta y_3 - \\ G(1 + \Delta\beta_{yx} - \Delta\beta_{yz}) \end{bmatrix} \right) dt$

4	$P_{a4x}=SF_{a4}(T)\int_0^T\left(b_{a4}(T)+\frac{1}{\sqrt{2}}\left[\begin{array}{l}G(\Delta\alpha_{yz}+\Delta\alpha_{yx})+\\ \omega_x^2\Delta y_4(1+\Delta\alpha_{yz}-\Delta\alpha_{yx})-\omega_x^2\Delta z_4\end{array}\right]\right)dt$ $P_{a4y}=SF_{a4}(T)\int_0^T\left(b_{a4}(T)+\frac{1}{\sqrt{2}}\left[\begin{array}{l}\omega_y^2(\rho+\Delta x_4)(\Delta\alpha_{yz}+\Delta\alpha_{yx})+\\ G(1+\Delta\alpha_{yz}-\Delta\alpha_{yx})-\omega_y^2\Delta z_4\end{array}\right]\right)dt$ $P_{a4z}=SF_{a4}(T)\int_0^T\left(b_{a4}(T)+\frac{1}{\sqrt{2}}\left[\begin{array}{l}\omega_z^2(\rho+\Delta x_4)(\Delta\alpha_{yz}+\Delta\alpha_{yx})+\\ \omega_z^2\Delta y_4(1+\Delta\alpha_{yz}-\Delta\alpha_{yx})-G\end{array}\right]\right)dt$
5	$P_{a5x}=SF_{a5}(T)\int_0^T\left(b_{a5}(T)+\frac{1}{\sqrt{2}}\left[\begin{array}{l}G(1-\Delta\beta_{zy})+\omega_x^2(\rho+\Delta y_5)\Delta\beta_{zx}-\\ \omega_x^2\Delta z_5(1-\Delta\beta_{zx}+\Delta\beta_{zy})\end{array}\right]\right)dt$ $P_{a5y}=SF_{a5}(T)\int_0^T\left(b_{a5}(T)+\frac{1}{\sqrt{2}}\left[\begin{array}{l}\omega_y^2\Delta x_5(1-\Delta\beta_{zy})+G\Delta\beta_{zx}-\\ \omega_y^2\Delta z_5(1-\Delta\beta_{zx}+\Delta\beta_{zy})\end{array}\right]\right)dt$ $P_{a5z}=SF_{a5}(T)\int_0^T\left(b_{a5}(T)+\frac{1}{\sqrt{2}}\left[\begin{array}{l}\omega_z^2\Delta x_5(1-\Delta\beta_{zy})+\omega_z^2(\rho+\Delta y_5)\Delta\beta_{zx}-\\ G(1-\Delta\beta_{zx}+\Delta\beta_{zy})\end{array}\right]\right)dt$
6	$P_{a6x}=SF_{a6}(T)\int_0^T\left(b_{a6}(T)+\frac{1}{\sqrt{2}}\left[\begin{array}{l}G(1-\Delta\alpha_{zy})-\omega_x^2\Delta y_6(1+\Delta\alpha_{zy}+\Delta\alpha_{zx})+\\ \omega_x^2(\rho+\Delta z_6)\Delta\alpha_{zx}\end{array}\right]\right)dt$ $P_{a6y}=SF_{a6}(T)\int_0^T\left(b_{a6}(T)+\frac{1}{\sqrt{2}}\left[\begin{array}{l}\omega_y^2\Delta x_6(1-\Delta\alpha_{zy})-G(1+\Delta\alpha_{zy}+\Delta\alpha_{zx})+\\ \omega_y^2(\rho+\Delta z_6)\Delta\alpha_{zx}\end{array}\right]\right)dt$ $P_{a6z}=SF_{a6}(T)\int_0^T\left(b_{a6}(T)+\frac{1}{\sqrt{2}}\left[\begin{array}{l}\omega_z^2\Delta x_6(1-\Delta\alpha_{zy})-\\ \omega_z^2\Delta y_6(1+\Delta\alpha_{zy}+\Delta\alpha_{zx})+G\Delta\alpha_{zx}\end{array}\right]\right)dt$

Assuming the original orientation errors, biases, scale factors and location errors shown in Tables 6 and 7. After calibrating the parameters of six-accelerometer, INS will be obtained and shown in Tables 8 and 9.

Table 6. The orientation errors, biases, scale factors of the six-accelerometer INS.

Number	Bias	Scale Factor	Orientation Error
1	0.001g	0.5	$\Delta\alpha_{xy}=0.6^o;\ \Delta\alpha_{xz}=0.5^o;$
4	0.001g	2.5	$\Delta\alpha_{yx}=0.8^o;\ \Delta\alpha_{yz}=0.7^o;$
6	0.001g	2.5	$\Delta\alpha_{zx}=0.4^o;\ \Delta\alpha_{zy}=0.8^o$
2	0.001g	2.5	$\Delta\beta_{xy}=0.6^o;\ \Delta\beta_{xz}=0.5^o;$
3	0.001g	0.5	$\Delta\beta_{yx}=0.8^o;\ \Delta\beta_{yz}=0.7^o;$
5	0.001g	2.5	$\Delta\beta_{zx}=0.4^o;\ \Delta\beta_{zy}=0.8^o$

Let the distance from the body-frame origin to each accelerometer be $\rho=0.1\text{m}$ and the vehicle motion with linear acceleration, angular acceleration are

$$\ddot{\vec{r}}^{\,i}=\left[9.81\quad 0\quad 0\right]^T \text{m}/\text{s}^2,$$

$$\dot{\vec{\omega}}_{ib}=\left[\pi/4\quad 0\quad 0\right]^T \text{rad}/\text{s}^2.$$

Table 7. The location errors of the six-accelerometer INS.

Number	Δx	Δy	Δz
1	0.5×10^{-3}m	0.8×10^{-3}m	0.6×10^{-3}m
2	0.7×10^{-3}m	0.5×10^{-3}m	0.6×10^{-3}m
3	0.5×10^{-3}m	0.9×10^{-3}m	0.8×10^{-3}m
4	0.4×10^{-3}m	0.7×10^{-3}m	0.5×10^{-3}m
5	0.8×10^{-3}m	0.7×10^{-3}m	0.5×10^{-3}m
6	0.6×10^{-3}m	0.8×10^{-3}m	0.9×10^{-3}m

All initial conditions for vehicle motion are zero.

The determined linear acceleration errors of vehicle, caused by original and calibrating orientation and location error, are shown as Figs. 5-7. The determined angular acceleration errors of vehicle, caused by original and calibrating orientation and location error, are shown as Figs. 8-10. These figures show that the linear and angular acceleration errors due to calibrating orientation and location error can approach to the acceleration errors due to original orientation and location error.

Table 8. The orientation errors, biases, scale factors on calibration.

Number	Bias	Scale Factor	Orientation Error
1	0.001g	0.5	$\Delta\alpha_{xy}=0.5930^o;\ \Delta\alpha_{xz}=0.5042^o;$
4	0.001g	2.4996	$\Delta\alpha_{yx}=0.8074^o;\ \Delta\alpha_{yz}=0.7001^o;$
6	0.001g	2.4997	$\Delta\alpha_{zx}=0.4000^o;\ \Delta\alpha_{zy}=0.8001^o$
2	0.001g	2.4998	$\Delta\beta_{xy}=0.5930^o;\ \Delta\beta_{xz}=0.5042^o;$
3	0.001g	0.4999	$\Delta\beta_{yx}=0.8074^o;\ \Delta\beta_{yz}=0.7001^o;$
5	0.001g	2.4997	$\Delta\beta_{zx}=0.4000^o;\ \Delta\beta_{zy}=0.8001^o$

Table 9. The location errors on location calibration.

Number	Δx	Δy	Δz
1	0.38×10^{-3} m	0.85×10^{-3} m	8.91×10^{-3} m
2	0.51×10^{-3} m	0.58×10^{-3} m	0.72×10^{-3} m
3	5.42×10^{-3} m	0.9×10^{-3} m	0.92×10^{-3} m
4	5.22×10^{-3} m	0.57×10^{-3} m	0.5×10^{-3} m
5	0.8×10^{-3} m	0.88×10^{-3} m	0.5×10^{-3} m
6	0.6×10^{-3} m	0.8×10^{-3} m	1.09×10^{-3} m

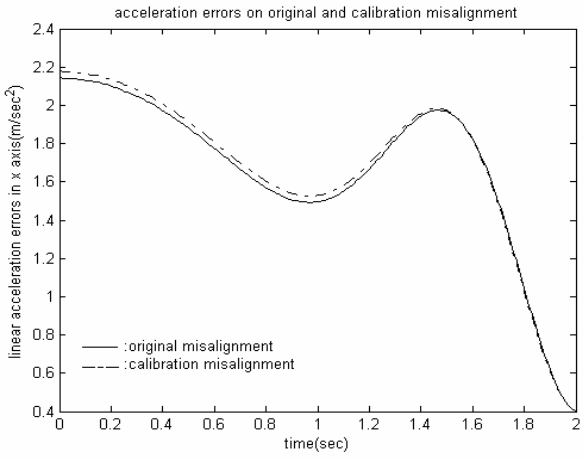

Fig. 5. The vehicle linear acceleration error in the x axis.

From Figs. 5-10 to know that the six-accelerometer INS error parameters can be obtained by proposed calibration method. The system errors contain the position error and orientation error of accelerometers.

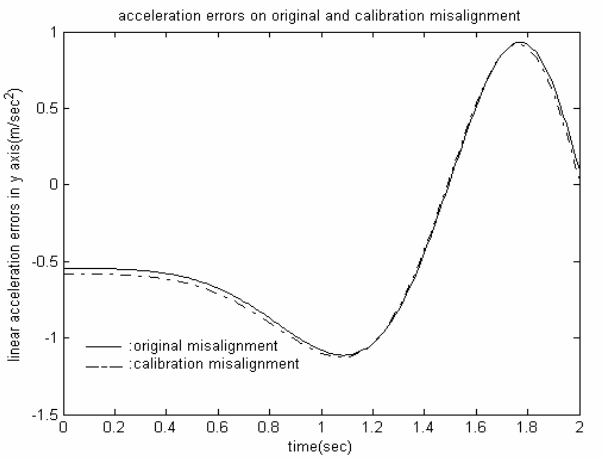

Fig. 6. The vehicle linear acceleration error in the y axis.

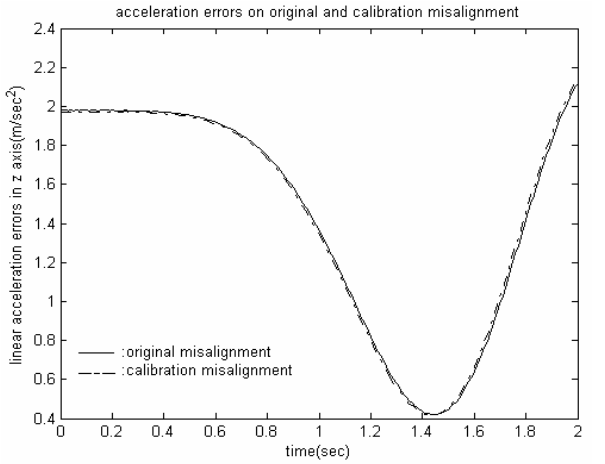

Fig. 7. The vehicle linear acceleration error in the z axis.

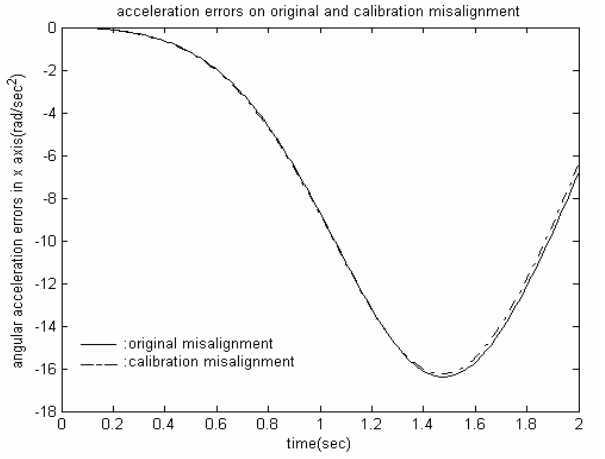

Fig. 8. The vehicle angular acceleration error in the x axis.

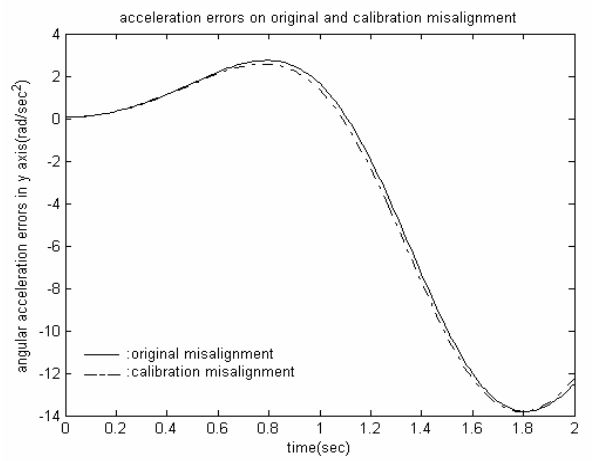

Fig. 9. The vehicle angular acceleration error in the y axis.

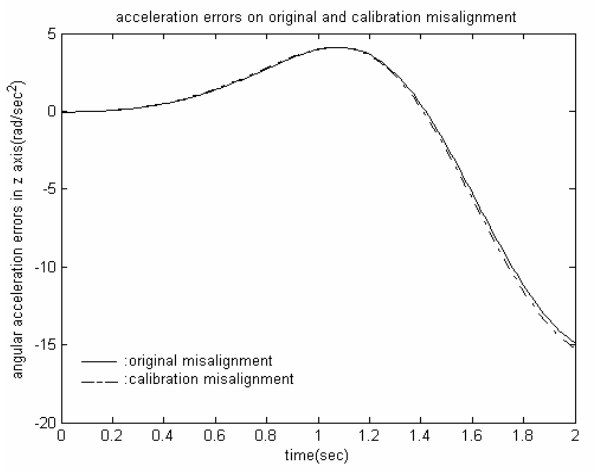

Fig. 10. The vehicle angular acceleration error in the z axis.

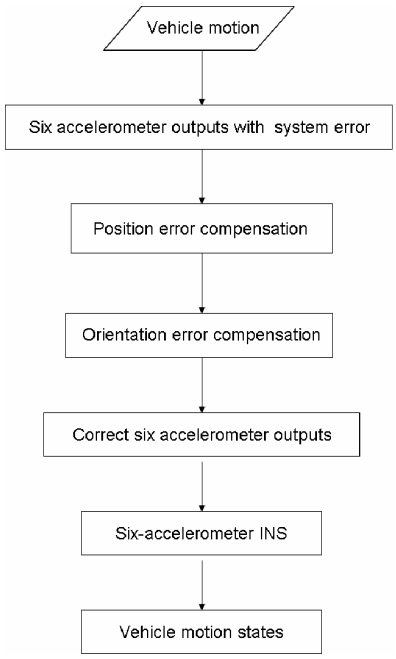

Fig. 11. The system error compensation flow chart.

The orientation error affects the accelerometer output accuracy. The position error affects the output accuracy when the vehicle takes rotation motion. In navigation application, its navigation precision can be enhanced by compensating position and orientation error. The flow chart is shown as Fig. 11.

6. CONCLUSION

The navigation accuracy of the six-accelerometer INS depends on bias, scale factor, orientation and location error. The proposed multi-position calibration proves a numerical method to obtain these error parameters in laboratory. From the simulation results know that the proposed multi-position calibration can find unique solution. On future we can use the error parameters to integrate the six-accelerometer INS with the GPS. It can increase the decision of navigation to apply on UAV, auto-pilot and guidance.

REFERENCES

[1] K. R. Britting, *Inertial Navigation System Analysis*, Chap. 8, pp. 153-195, Wiley-Interscience, New York, 1971.

[2] C. F. O'Donnell, "Inertial navigation," *J. of the Franklin Institute*, vol. 266, no. 4-5. Oct.-Nov. 1958.

[3] L. D. DiNapoli, *The Measurement of Angular Velocities Without the Use of Gyros*, M. S. Thesis, The Moore School of Elec. Engineering, University of Pennsylvania, Aug. 1965.

[4] A. R. Schuler, A. Grammatikos, and K. A. Fegler, "Measuring rotational motion with linear accelerometers," *IEEE Trans. on Aerospace and Electronic Systems*, vol. AES-3 no. 3, pp. 465-471, May 1967.

[5] J. H. Chen, S. C. Lee, and D. B. DeBra, "Gyroscope free strapdown inertial measurement unit by six liner accelerometers," *Journal of Guidance, Control, and Dynamics,* AIAA, vol. 17, no. 2, pp. 286-290, March-April 1994.

[6] K. Mostov, C. W. Tan, and P. Varaiya, "Development of integrated navigation systems based on gryo-free INS," *U.C. Berkeley PATH Lab. Report.* Available: http://www.path.berkeley.edu/PATH/Research/1999_progwide/ 07.pdf

[7] C. W. Tan, K. Mostov, and P. Varaiya, "Feasibility of a gyroscope-free inertial navigation system for tracking rigid body motion," *California PATH Research Report*, *UCB-ITS-PRR-2000-9*, May 2000.

[8] C. W. Tan and S. Park, "Design and error analysis of accelerometer-based inertial navigation systems," *California PATH Research Report*, *UCB-ITS-PRR-2002-21*, June 2002.

[9] W. Wrigley, W. M. Hollister, and W. G. Denhard, *Gyroscopic Theory, Design, and Instrumentation*,

Chap. 12, pp. 241-242, The Massachusetts Institute of Technology Press, 1969.

Chao-Yu Hung received the B.S. from Chinese Military Academy in 1988 and the M.S. degree in Engineering Science from National Cheng Kung University 1996. He is currently working toward a Ph.D. degree at Department of a System Engineering, Chung Cheng Institute of Technology, National Defense University, Taiwan, His research interests include Integrated Navigation System, INS, GPS, calibration and error analysis.

Sou-Chen Lee received the B.S., M.S., and Ph.D. degrees in System Engineering from Chung Cheng Institute of Technology in 1979, 1985, and 1993 respectively. Since 2004, he has been a Dean of College of Electrical Engineering and Computer Science, Lunghwa University. His research interests include dynamic system, INS and guidance.